

The relationship between reinforcing index and flexural parameters of new hybrid fiber reinforced slab

Mingli Cao^a, Chaopeng Xie^{*}, Li Li and Mehran Khan

School of Civil Engineering, Dalian University of Technology,
Linggong Road, Ganjingzi District, Dalian, People's Republic of China

(Received May 23, 2018, Revised November 12, 2018, Accepted November 16, 2018)

Abstract. In this paper, a new hybrid fiber system (NHFS) is investigated for the application of slab. The steel fiber, polyvinyl alcohol (PVA) fiber and calcium carbonate (CaCO_3) whisker is added to form NHFS. The four-point bending test is carried out on the flexural properties of slab with plain, steel fiber, traditional hybrid fiber system (THFS) and NHFS reinforced cementitious composites. The flexural behavior is evaluated by ASTM C1018-97, JCI-SF4 and post-crack strength (PCS) technique. The evaluation parameters of flexural toughness such as toughness index (TI), equivalent flexural strength (EFS) and PCS are determined. The size of slab specimens is 15 mm (thickness) \times 50 mm (width) \times 200 mm (length). The results show that adding CaCO_3 whisker to THFS can significantly improve the flexural strength, TI, EFS, PCS of the slab. The empirical relation between reinforcing index (RI_v) and flexural parameters show that flexural parameters of slabs increase first and then decrease; which indicates that optimum RI_v values can be helpful in the considering the mix design of steel-PVA fibers- CaCO_3 whisker composites for achieving the desired flexural-related properties. The scanning electron microscopy is performed to observe the micro-morphological characteristics of the fracture surface, which proved the positive hybrid effect among the different fibers in cementitious composites. The NHFS can arrest the generation and propagation of the crack from micro to macro level.

Keywords: new hybrid fiber system; slab; CaCO_3 whisker; flexural toughness; reinforcing index; scanning electron microscopy

1. Introduction

To control the cracking in cementitious composites is an important aspect in the construction industry nowadays. The structures of cementitious composites have prominent multilevel characteristic which determines the multilayer characteristics of its destruction process (Pichler *et al.* 2018, Pereira *et al.* 2012). Fibers are usually added into cementitious composites to improve the resistance against cracking and solve the shortcoming of high brittleness and low ductility of matrix effectively. (Arslan 2016, Alberti *et al.* 2016, Kazemi *et al.* 2017, Tuan *et al.* 2017). Nowadays, many kinds of fibers i.e., metallic, polymeric, natural fibers are used widely in cementitious composites to arrest cracking (Abadel *et al.* 2015, Kim *et al.* 2013). However, none of these single fiber can control cracks at full scales. The proposed hybrid fiber system concept is a good way to control cracks at different scales, such as the large and the strong fibers is used to resist crack at macro scale; the small fiber is used to control crack at micro scale (Qian and Stroeven 2000, Soleimani and Banthia 2005). Steel fiber is a strong and stiff fiber which could collaborate with cementitious composites and have the excellent ability of

crack arresting (Soleimani and Banthia 2005, Najjigivi *et al.* 2017). The polyvinyl alcohol fiber (PVA) is a small and soft fiber whose surface covered with hydroxyl which have a good bond behavior with matrix and can control the propagation of cracks, and decentralize the cracks on the meso-level (Cao *et al.* 2017). Therefore, steel-PVA hybrid fiber system has been used traditionally to reinforce cementitious composites (THFRCC) (Sun *et al.* 2001, Zhang *et al.* 2017, Yun *et al.* 2007, Lawler *et al.* 2016).

In recent years, Cao *et al.* (2013, 2014a) introduce a new type of inorganic micro fiber calcium carbonate (CaCO_3) whisker with good characteristic i.e., high tensile strength, high elastic modulus, low price and large aspect ratio which had been used in cementitious composites, and showed a good crack resistance behavior at the micro level. The CaCO_3 whisker of micron scale not only can arrest the generation and development of micro crack, but also fill the pores in the matrix (Cao *et al.* 2013). Nowadays, adding CaCO_3 whisker into traditional hybrid fiber system (THFS) to form a new hybrid fiber system (NHFS) can help to control the multilevel cracking in cementitious composites. The mechanical properties like tensile strength, toughness and the shrinkage performance were improved by using NHFS (Cao *et al.* 2014b, Cao *et al.* 2015). Meanwhile, CaCO_3 whisker partial substitution with steel fiber and PVA fiber can bring good economic benefits, because of lower cost of CaCO_3 whisker (approximately \$230 per ton) than that of steel fiber and PVA fiber (Cao *et al.* 2015).

Nowadays, the engineering applications of fiber reinforced cementitious composites (FRCC) mainly focused

*Corresponding author, Ph.D. Student
E-mail: xie_chaopeng@mail.dlut.edu.cn

^aAssociate Professor
E-mail: minglic@dlut.edu.cn

the flexural members which have relatively thin features like bridge decks (Khan and Ali 2016), connecting slabs of bridge, repair of structural components (Li 2007), pavements (Cao *et al.* 2014) and protective outer walls (Atahan *et al.* 2013). Slabs are the typical flexural member, and a large number of researchers have reported the flexural performance of FRCC. Demir (2015) predicted the compression strength and flexural strengths of hybrid fiber reinforced concrete by an artificial neural network (ANN) model which developed by the author. The comparison results between predicted values and experimentally measured values showed a good consistency. Said *et al.* (2015a) studied the flexural response of engineered cementitious composite (ECC) slab with PVA fiber. The flexural toughness was evaluated by ASTM C1018 standard and post-crack strength (*PCS*) technique. The results indicated that with increase in reinforcing index (*RI*), the value of toughness indices (*TI*) and *PCS* values increases. Said and Razak (2015b) also investigated the flexural behavior of engineered cementitious composite (ECC) slabs with polyethylene fiber. It was found that, as the *RI* value increased, the *TI* also significantly increased. The increased *PCS* values showed good flexural behavior i.e., better deformability and higher energy absorption capacity. Khan and Ali (2016) used glass and nylon fibers reinforced concrete to control early cracking of concrete bridge decks. The result showed that the flexural strengths of glass fiber reinforced concrete (GFRC) and nylon fiber reinforced concrete (NFRC) was improved, as compared to that of plain concrete. Although the energy absorption of GFRC and NFRC was less before cracks appeared, but their post-cracking behavior and *TI* value were more than that of plain concrete. Ahmed *et al.* (2007) studied the flexural properties of hybrid steel-polyethylene fiber reinforced cementitious composites containing high volume fly ash using four-point bending test. The highest flexural strength was achieved at 1.0% steel with 1.5% polyethylene fibers. The 0.5% steel and 2.0% polyethylene fibers had the highest flexural toughness. Although all of above studies reported that the addition of fibers could improve the flexural behavior of slabs, none of them involved the micro fiber. Therefore, it is necessary to study the flexural properties of slabs with micro fiber reinforced cementitious composites to better understand the behavior for structural applications.

The previously published article (Cao *et al.* 2015) focus on properties of beams but the attention was not given to slabs. The influence of fibers in slabs may be significantly different, so the slab needs to be investigated in order to predict real behavior for engineering applications. To the best of author's knowledge, no study has been reported on flexural properties of slab with combination of steel, PVA fibers and CaCO_3 whisker for controlling cracking. In this paper, the flexural properties of slab with the plain cementitious composites, steel fiber reinforced cementitious composites (steel fiber+PVA fiber) and new hybrid fiber reinforced cementitious composites (steel fiber+PVA fiber+ CaCO_3 whisker) are investigated. The flexural toughness of slab is evaluated by ASTM C1018, JCI-SF4 and *PCS* techniques. In addition to this, the empirical

Table 1 Chemical composition of cement and CaCO_3 whisker (wt.%)

Composition	CaO	SiO ₂	Al ₂ O ₃	Fe ₂ O ₃	CO ₂	MgO	K ₂ O	SO ₃	Na ₂ O	P ₂ O ₅	MnO
Cement	61.13	21.45	5.24	2.89	2.37	2.08	0.81	2.50	0.77	0.07	0.06
Whisker	54.93	0.29	0.11	0.07	42.07	2.14	-	0.31	-	-	-

Table 2 Properties of raw materials

Material name	Density (g·cm ⁻³)	Size	Mechanical property
Cement	3.2	Specific surface area 356 m ² /kg	-
Silica sand	2.65	Fineness modulus 1.9	Moh's hardness 7
Steel fiber	7.8	Length 13 mm	Tensile strength ≥ 2000 MPa
		Diameter 200 μm	Elastic modulus 210 GPa
PVA fiber	1.29	Length 12 mm	Tensile strength 1600 MPa
		Diameter 31 μm	Elastic modulus 39 GPa
CaCO_3 whisker	2.86	Length 20-30 μm	Tensile strength 3000-6000 MPa
		Diameter 0.5-2 μm	Elastic modulus 410-710 GPa

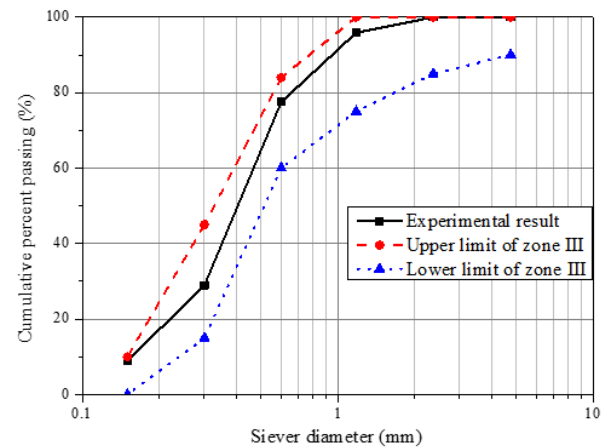


Fig. 1 Grading curve of silica sand used in the research

relation between *RI* and evaluation parameters of flexural toughness are developed. The flexural strength, *RI*, *TI*, equivalent flexural strength and post-crack strength are explored and discussed in detail.

2. Experimental and program

2.1 Materials

An ordinary Portland cement (P·O 42.5R) is used. The chemical compositions and properties of raw material are shown in Tables 1-2, respectively. The fine aggregate is ordinary silica sand and the properties are presented in Table 2. The grading curve of silica sand is presented in Fig. 1. CaCO_3 whiskers were provided by Youxing Technology Co. Ltd. (Changde, China), and their chemical composition is also shown in Table 1. Smooth and straight PVA fibers were acquired from Kuraray China Co., Ltd. Steel fibers were from Bekaert OL. The mechanical properties and morphologies are presented in Table 2 and Fig. 2, respectively. The mixing water is ordinary tap water. Based on previous findings (Cao *et al.* 2014b, Cao *et al.* 2015), the water cement ratio was kept as 0.3 and the sand cement

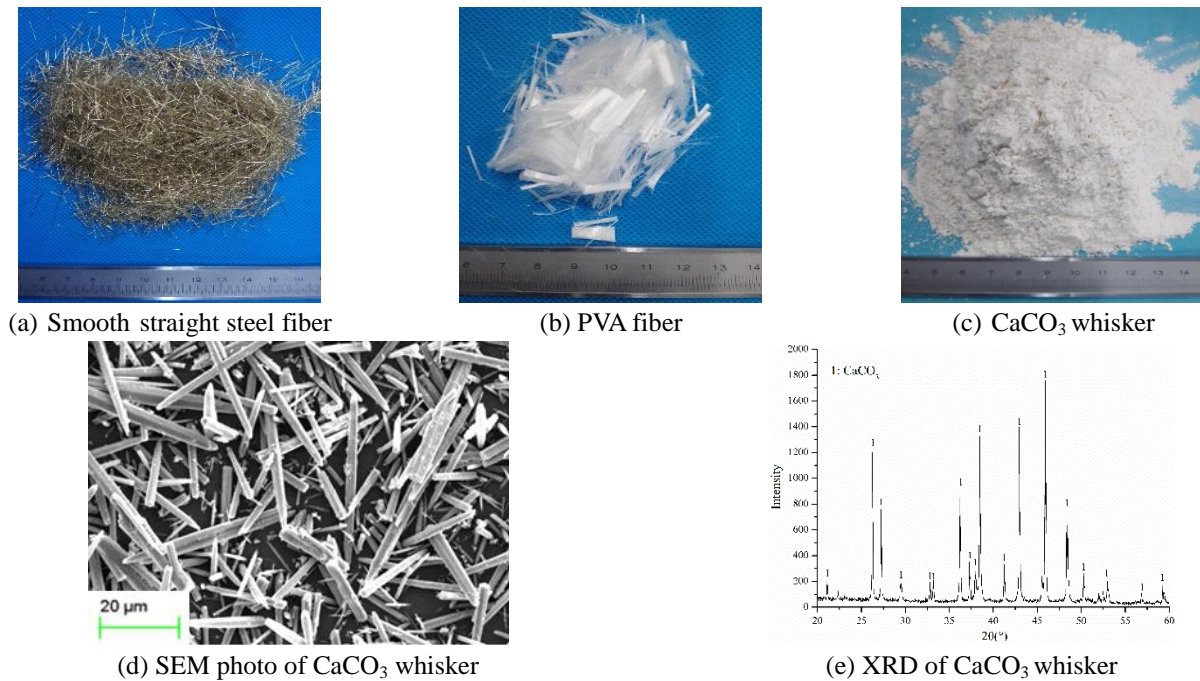


Fig. 2 Morphologies of fibers used in the study

Table 3 Mixing dosage of different fiber combinations

Groups		Volume fraction/%			Fiber dosage/(kg/m ³)		
		Steel fiber	PVA fiber	CaCO ₃ whisker	Steel fiber	PVA fiber	CaCO ₃ whisker
Control	plain	0.00	0.00	0.00	0	0	0
	SF*	2.00	0.00	0.00	156	0	0
Traditional hybrid system	THFS-1	1.75	0.25	0.00	136.5	3.225	0
	THFS-2	1.50	0.50	0.00	117	6.450	0
	THFS-3	1.25	0.75	0.00	97.5	9.675	0
	THFS-4	1.00	1.00	0.00	78	12.90	0
New hybrid system	NHFS-1	1.75	0.20	0.50	136.5	2.580	14.3
	NHFS-2	1.50	0.40	1.00	117	5.160	28.6
	NHFS-3	1.25	0.55	2.00	97.5	7.095	57.2
	NHFS-4	1.00	0.70	3.00	78	9.030	85.8

*SF: Steel fiber; THFS: (Steel + PVA) fibers; NHFS: (Steel + PVA) fibers and CaCO₃ whisker.

ratio was controlled to 0.5. The mixing dosage of all groups with different fiber combinations is shown in Table 3 and these fibers ratios are selected based on the previous studies (Cao *et al.* 2015, Zhang and Cao 2014).

The polycarboxylate water reducer is used. To provide a good workability for fresh mixture, the dosage of the water reducer is controlled within 0.5wt%-1.5wt%, and the flow ability is also measured. The result of flow ability of fresh mixture is stated in Table 4.

2.2 Test specimens

First of all, raw material i.e., cement, sand, CaCO₃ whisker are poured into blender and mix it for thirty seconds to make the dry material homogenous. Then water and water reducer is added to form cement mortar. After that, steel fiber and PVA fiber are added into the mortar,

Table 4 The amount of water reducer and flow ability of fresh matrix

Groups	Water reducer dosage/(g)	Flow spread values/(cm)
Plain	3	23
SF	3.3	19.5
THFS-1	4.8	22.5
THFS-2	4.3	19
THFS-3	5.8	21
THFS-4	8	25.8
NHFS-1	3.8	25
NHFS-2	5.0	24
NHFS-3	6.6	23
NHFS-4	11	25

respectively, and start mixing to ensure uniform dispersion of fibers. At the last process of mixing, the fixed amount of defoaming agent (1ml tributyl phosphate) is added, and its aim was to eliminate the bubbles that are formed by the addition of fibers. The addition of excess defoaming agent always lead to the changes of workability. However, a small amount of defoaming agent cannot achieve a good anti-foaming effect. The flow chart of mixing process of raw materials is shown in Fig 3. To ensure the uniform distribution of PVA fiber, the mixing time in step four was kept sixty seconds. Almost the all the material was mixed in the blender so the mixing time was 15 seconds after the addition of deformer.

After mixing, the fresh mixture is poured into the steel molds having dimension of 15 mm×50 mm×200 mm and vibrator is used to ensure compactibility. After that, these specimens are placed with steel molds in the mortar standard curing box. After 24 hours, these specimens are demolded and cured for 28 days in water at 20°C.

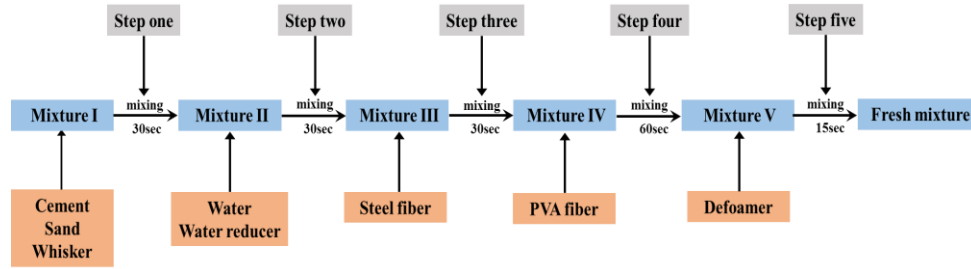
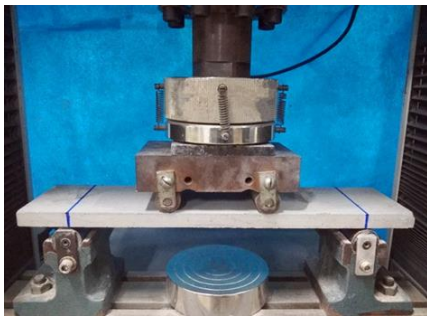
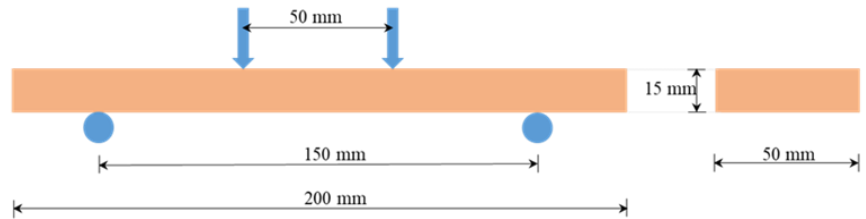


Fig. 3 The mixing process of materials



(a) Four-point bending during testing



(b) Schematic diagram

Fig. 4 Loading diagram of slab

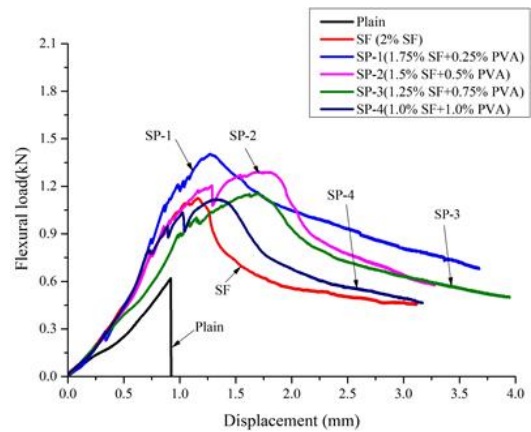
2.3 Flexural test

The four-point bending test was performed to determine the flexural properties of slabs. The microcomputer controlled electronic universal testing machine WDW-10E was used with displacement controlled having loading rate of 0.1 mm/min in the flexural test (Cao *et al.* 2017). The span length of the flexural specimen was 150 mm. In the experiment, the value of load and deflection were recorded, respectively. The experimental setup of four-point bending during testing is shown in Fig. 4(a) and the schematic diagram is shown in Fig. 4(b). Steel fiber group, steel and PVA fibers group and steel, PVA fibers and CaCO₃ whisker group are denoted by SF, THFS, and NHFS, respectively. Average of three values are taken for each property.

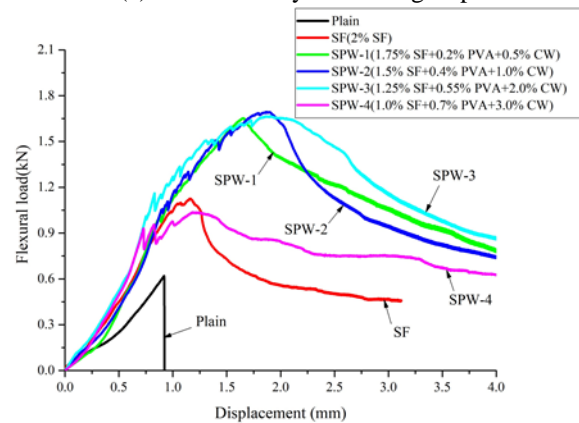
3. Results and analysis

3.1 Flexural load-deflection curves

The flexural properties of slabs with different kinds of hybrid fiber reinforced cementitious composites are evaluated, and the load-deflection curves are shown in Fig. 5(a)-(b). From Fig. 5(a)-(b), the plain group presents brittle failure, and it has the lowest flexural load value and the less deflection capacity among all other groups. On the other hand, the group with SF and hybrid fiber has a better flexural performance than plain group. Fig. 5(a) exhibits that the groups with the THFS not only have a higher load, but also have a better deflection capacity, as compared with that of plain and SF groups. The reason for these increase may be due to the steel-PVA fiber have synergy effect on the flexural load and deflection of cementitious composites. The synergy effect can be explained that PVA fiber could



(a) Traditional hybrid fiber group



(b) New hybrid fiber group

Fig. 5 The load-deflection curves

play a role in restricting the cracks at mesoscale; steel fibers were mainly used to prevent cracks by making a bridging effect at macroscale. As thus, steel-PVA hybrid fiber could

arrest cracks at meso-macro levels. Meanwhile, it should be pointed out that the synergy effect between steel fiber and PVA fiber is greater than superimposed effect among two. Among the curves of THFS, THFS-1 group possess the highest ultimate load than the others, but its corresponding deflection value is less than that of THFS-2, THFS-3, THFS-4. However, it may be noted that the deflection value is also higher than that of plain and SF groups. This may be interpreted that PVA fiber can improve the deflection ability of hybrid fiber reinforced cementitious composites more efficiently than that of steel fiber (Zhang and Cao 2014). There are no enough PVA fiber to bridging matrix when small cracks appearance at mesoscale in THFS-1 group.

Fig. 5(b) shows that the curves of NHFS have more extended softening behavior and deformation capacity after peak load than that of THFS. The addition of CaCO₃ whisker to steel- PVA hybrid fiber reinforced cementitious composites have a positive impact on the specimens in flexural behavior. Especially, in NHFS, the NHFS-1, NHFS-2 and NHFS-3 have extremely excellent capacity with improved flexural load and deflection capacity. This may be due to the effect of NHFS which play a multilevel action of cracking resistance at different scales. In NHFS, CaCO₃ whisker can fill the pores in matrix and make a key role in restraining cracking and delaying the development of cracks by means of whisker pulled out, cracks deflection and cracks bridge mechanism (Cao *et al.* 2014a, Cao *et al.* 2014b). However, NHFS-4 is different from NHFS -1, NHFS-2 and NHFS-3. The reason is that the higher content of PVA fiber and CaCO₃ whisker result in poor dispersion and matrix defect (Zhang and Cao 2014). To compare all curves in Fig. 5(a)-(b), that can be easily observed that the hybrid fiber groups are superior to the plain and SF groups. And CaCO₃ whisker partially replacing with PVA fiber in NHFS present best flexural behavior. It may be concluded that there exists positive hybrid effect among steel fiber, PVA fiber and CaCO₃ whisker with various proportion, and the positive hybrid effect in NHFS have improved flexural properties than that of THFS. The fiber combination in NHFS-3 group demonstrate the best positive hybrid effect than that of other groups. The positive hybrid effect could be illuminated that the addition of micron-sized CaCO₃ whisker was able to inhibit or delay the generation, evolution and growth of cracks at microscale. Meanwhile, steel fiber and PVA fiber could make an effect on macro and meso scales, respectively. So, steel fiber, PVA fiber and CaCO₃ whisker can develop their own advantages at multiscale in cementitious composites. Moreover, the positive hybrid effect in the paper is not simply superimposed effect among three, but greater than the sum of the superposition. For instance, the addition of CaCO₃ whisker not only could fill the pores in cementitious composites, but also could improve matrix compactness which can contribute to improving the bonding capacity between fiber and matrix ultimately resulting in positive hybrid effect.

3.2 Reinforcing index

The reinforcing index (RI_v) is a main parameter to

evaluate the effect of fiber in cementitious composites and have close relationship with fiber content and aspect ratio (Abadel *et al.* 2015, Said *et al.* 2015a, b). For single fiber, CECS38 (2004) define a λ_f as characteristic value of steel fiber, which is as follows

$$\lambda_f = \rho_f \times \frac{l_f}{d_f} \quad (1)$$

Where, ρ_f represent volume fraction of fiber, l_f represent fiber length and d_f represent fiber diameter.

For hybrid fiber, since different fiber characteristics are present, so only some simple superposition is not enough. Hence, Almusallam *et al.* (2016), Cao and Li (2018) reported a sum of different fiber reinforcing index, which is as follows

$$RI_v = \sum_i^n k_i v_{fi} \frac{l_i}{d_i} \left(\frac{f_i}{f_s} \right)^\eta \quad (2)$$

Where, RI_v is the value of hybrid fibers reinforcing index. The suffix i represent fiber type. The value of i is taken as 1,2,3, where 1 is for steel fiber; 2 is for PVA fiber and 3 is for CaCO₃ whisker. k_i represent the mechanical anchoring coefficient which has related to the surface shape of fiber. In this paper, the surface shape of steel fiber, PVA fiber and CaCO₃ whisker is smooth and straight, and have weak bonding with matrix. Thus, the k_i value of steel fiber, PVA fiber and CaCO₃ whisker are all taken as 0.1. Moreover, k_i was selected as reported by Almusallam *et al.* (2016), Cao and Li (2018). v_{fi} , l_i , d_i represent volume fraction of fiber, fiber length and fiber diameter, respectively. f_i is the tensile strength of different fiber type, and f_s is the tensile strength of steel fiber. The index η in Eq. (2) is the parameter that is related to fiber type, and for steel fiber it is 1, PVA fiber and CaCO₃ whisker both are all taken as 0.5 according to Almusallam *et al.* (2016) and Cao and Li (2018). Table 5 show the value of RI_v for all groups. The RI_v value of THFS-1, THFS-2, THFS-3, THFS-4, NHFS-1, NHFS-2, NHFS-3 and NHFS-4 are increased by 15.8%, 31.6%, 47.3%, 63.1%, 30.3%, 60.6%, 105.5% and 150.3% respectively, as compared to that of SF group.

3.3 Flexural strength

According to ASTM C1018 (1997), the first crack point on the load-deflection curve is the point when the curve first becomes nonlinear (approximates the onset of cracking in the concrete matrix). The flexural strength can be calculated based on ASTM C1609/1609M (2012) and the results are presented in Table 5. The Eq. (3) is presented as follow

$$\sigma = \frac{PL}{bh^2} \quad (3)$$

Where P is the load value, L is the span length, b is the width of slabs, and h is the thickness of slab.

The value of first crack strength, ultimate strength, and relative increase ratio are compared with SF group which reflect the degree of hybrid fiber improvement of strength to that of single fiber and are shown in Table 5. Fig. 6 presents the comparison of flexural strength of plain, SF,

Table 5 Reinforcing index, first crack strength and ultimate strength

Groups	RI_v	σ_{cr} (MPa)	σ_u (MPa)	$\sigma_{cr-i}/\sigma_{cr-s}$	$\sigma_{u-i}/\sigma_{u-s}$
plain	0	8.253	8.253	0.786	0.550
SF	0.130	10.493	14.999	1	1
THFS -1	0.200	11.447	18.731	1.091	1.249
THFS -2	0.271	12.609	17.240	1.202	1.149
THFS -3	0.341	11.481	15.390	1.094	1.026
THFS -4	0.411	10.485	14.916	0.999	0.994
NHFS -1	0.209	13.569	22.033	1.293	1.469
NHFS -2	0.288	13.937	22.584	1.328	1.506
NHFS -3	0.377	14.008	22.203	1.335	1.480
NHFS -4	0.465	12.653	13.829	1.206	0.922

Note: σ_{cr} is first crack strength; σ_u is ultimate strength; σ_{cr-i} is the first crack strength value of different groups; σ_{u-i} is ultimate strength value of different groups; σ_{cr-s} is the first crack strength value of SF group; σ_{u-s} is ultimate strength value of SF group;

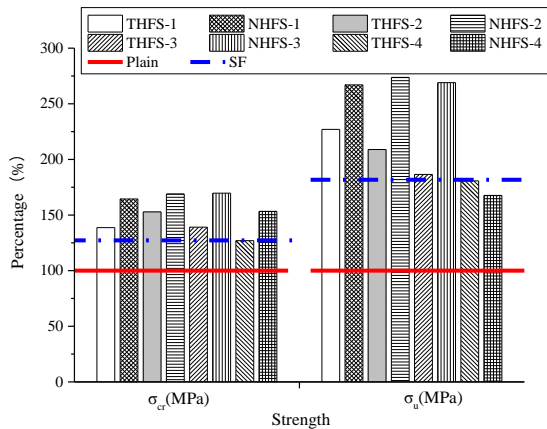


Fig. 6 Comparison of flexural strength of plain, SF, THFS and NHFS groups

THFS, NHFS groups. Plain group has the lowest flexural strength than that of SF, THFS, NHFS groups. All of the hybrid fiber groups except THFS-4 and NHFS-4 showed greater flexural strength than that of plain and SF groups. The first crack strength of THFS-1, THFS-2, THFS-3, THFS-4, NHFS-1, NHFS-2, NHFS-3 and NHFS-4 are increased by 9.1%, 20.2%, 9.4%, 0%, 29.3%, 32.8%, 33.5% and 20.6%, respectively, as compared to that of SF group. The ultimate strength of THFS-1, THFS-2, THFS-3, NHFS-1, NHFS-2 and NHFS-3 are increased by 24.9%, 14.9%, 2.6%, 46.9%, 50.6% and 48.0% respectively, as compared to that of SF group. The reason for increased strength may be due to the positive hybrid effect between fiber and whisker to control the development of cracks in cementitious composites and also reported by Cao *et al.* (2014a). While THFS-4 and NHFS-4 are decreased by 1% and 8%, respectively. This may be due to high volume fraction of PVA fiber result in balling effect and poor dispersion, and where as the excessive amount of CaCO₃ whisker also brought some internal defects to matrix (Cao *et al.* 2013). The first crack strength of NHFS-1, NHFS-2, NHFS-3 and NHFS-4 are improved by 18.5%, 10.5%,

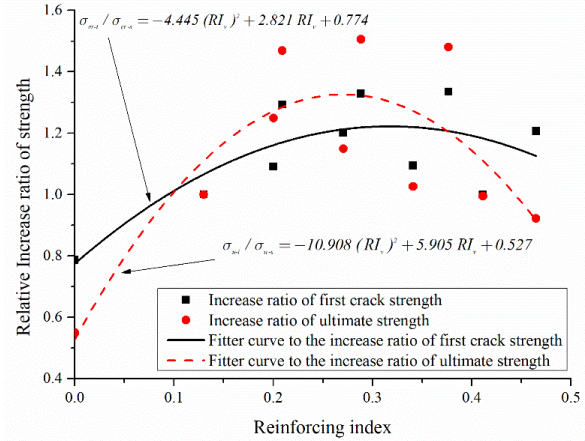


Fig. 7 Relationship between reinforcing index and relative increase ratio of strength

22.0% and 20.7%, respectively, as compared to that of THFS-1, THFS-2, THFS-3, THFS-4, respectively. This may be due to smaller length, higher tensile strength and high aspect ratio CaCO₃ whisker addition into steel-PVA hybrid fiber reinforced cementitious composites. The PVA fiber play role in arresting cracks at mesoscale, and CaCO₃ whisker inhibit the initiation, development and propagation of micro-cracks of cracks at microscale (Cao *et al.* 2015). The test results also show using CaCO₃ whisker partial substitute PVA fiber in NHFRS can improve flexural strength and achieve economic effectiveness in engineering application.

Fig. 7 shows that the fitting curves are quadratic function. The fitting curves give trend information. The increase ratio of first crack strength and ultimate strength seems gradually increases in the start and then decreases with the increase in reinforcing index values. This shows that the optimum fiber content or aspect ratio value can improve the strength. On the other hand, the excessive fiber content may lead to less homogeneity and low workability of mixture, which results in decreased strength. The fitting formulas are as follows:

For fitting curve of the increase ratio of first crack strength

$$\sigma_{cr-i} / \sigma_{cr-s} = -4.445(RI_v)^2 + 2.821RI_v + 0.774 \quad (4)$$

For fitting curve of the increase ratio of ultimate crack strength

$$\sigma_{u-i} / \sigma_{u-s} = -10.908(RI_v)^2 + 5.905RI_v + 0.527 \quad (5)$$

3.4 Flexural toughness

3.4.1 Evaluation of flexural toughness based on ASTM C1018

The flexural toughness is areas under the load-deflection curve up a specified deflection which is the energy absorption capacity of the test specimen according to ASTM C1018-97. The toughness index (*TI*) is stipulated as another important evaluation parameter to reflect the post-crack behavior under static flexural loading. The toughness

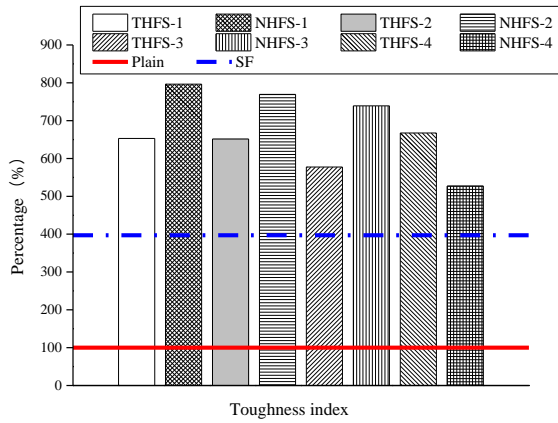


Fig. 8 Comparison of toughness index of plain, SF, THFS and NHFS groups

index express flexural performance from first crack deflection to a specified deflection in load-deflection curve. The Eq. (6) is as follows

$$TI_i = \frac{T_i}{T_c} \quad (6)$$

Where the T_c and T_i are the energy absorption capacities in the first crack deflection and specified deflection, respectively. The value of T_c and T_i are the corresponding area under the load-deflection curves. According to ASTM C1080, the value of i can be 5, 10, 20. However, it should be noted that $i=5$ refer to 3 times first crack deflection (3δ), TI_5 is the ratio of the area at 3.0 times first crack deflection to the area at first crack deflection. The TI_{10} and TI_{20} are similar to TI_5 , if $i=10$ or $i=20$ that means the area up to a deflection of 5.5 or 10.5 times the first-crack deflection by the area up to first crack. Since the limited deflections of specimens are not reach to 5.5δ or 10.5δ in this study, so only TI_5 is calculated.

From Fig. 8, plain group has lowest TI value, because of the brittle behavior. In comparison to SF group, the TI value of THFS-1, THFS-2, THFS-3, THFS-4, NHFS-1, NHFS-2, NHFS-3 and NHFS-4 are increased by 64.5%, 64.1%, 45.5%, 68.1%, 100.6%, 93.8%, 86.2% and 32.8%, respectively. The NHFS have higher TI value than THFS except NHFS-4. The TI value of NHFS-1, NHFS-2 and NHFS-3 are improved by 22.0%, 18.1% and 28.0%, respectively, as compared to that of THFS-1, THFS-2 and THFS-3, respectively. The reason may be that the addition of $CaCO_3$ whisker can fill in the pores and improving the density of matrix. On the other hands, $CaCO_3$ whisker as a micro fiber could control the generation and evolution of micro cracks. The TI value of NHFS-4 is lower than that of other NHFS, because the 0.7% PVA and 3% $CaCO_3$ whisker may result in poor dispersibility and bring internal defects to matrix ultimately has less TI . Fig. 9 shows the variation of TI_5 against the RI_v . The fitting curve is plotted and the correlation coefficient is 0.9 in the regression equation. It indicates that there exists a good correlation between the RI_v and TI_5 , and the analytical equation which given is fit for plain, SF, THFS and NHFS groups. The fitting formula is as follows

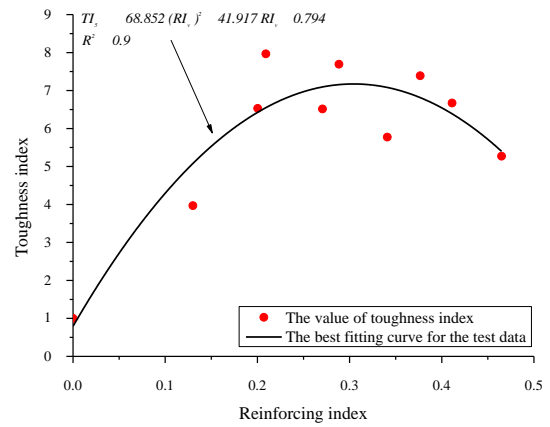


Fig. 9 Relationship between reinforcing index and toughness index

Table 6 Flexural toughness and equivalent flexural strength based on JCI-SF4

Group	Flexural toughness			Equivalent flexural strength		
	T_{b1} (N·m)	T_{b2} (N·m)	T_{b3} (N·m)	σ_{b1} (MPa)	σ_{b2} (MPa)	σ_{b3} (MPa)
Plain	0.24	0.24	0.24	3.25	2.17	1.08
SF	0.49	0.97	1.79	6.48	8.61	7.95
THFS -1	0.52	1.18	2.68	6.89	10.46	11.89
THFS -2	0.48	1.06	2.48	6.33	9.38	11.01
THFS -3	0.40	0.91	2.20	5.34	8.08	9.76
THFS -4	0.48	1.01	1.99	6.42	9.01	8.84
NHFS -1	0.47	1.14	3.09	6.22	10.11	13.74
NHFS -2	0.48	1.16	3.13	6.42	10.35	13.89
NHFS -3	0.59	1.31	3.56	7.84	11.61	15.81
NHFS -4	0.51	1.01	2.21	6.75	8.95	9.84

Note: T_{b1} , T_{b2} and T_{b3} is flexural toughness at the deflection of $L/150$, $L/100$ and $L/50$, respectively.

σ_{b1} , σ_{b2} and σ_{b3} is equivalent flexural strength at the deflection of $L/150$, $L/100$ and $L/50$, respectively.

$$TI_5 = -68.852 (RI_v)^2 + 41.917 RI_v + 0.794 \quad (7)$$

3.4.2 Evaluation of flexural toughness based on JCI-SF4

To evaluate flexural toughness of FRCC, the energy absorption capacity is calculated based on JCI-SF4 (1983). The values of flexural toughness are determined by calculating the area under the load-deflection curve up to a specific deflection. In this study, $L/150$, $L/100$ and $L/50$ are defined as the value of specific deflection, where L is the span of the specimens. Table 6 showed the value of flexural toughness of all groups. The hybrid fiber groups have a better flexural toughness than SF and plain group. The flexural toughness of hybrid fiber groups did not have significantly enhance at $L/150$ point, as compared to SF group. This is because of the small deflection in elastic stage which do not reach to first crack point, and fibers and whisker have not play an obvious effect. However, with increase in the deflection and after first crack appeared, the flexural toughness of hybrid fiber groups exceeded the SF group at $L/100$ and $L/50$ points. This may be due to the

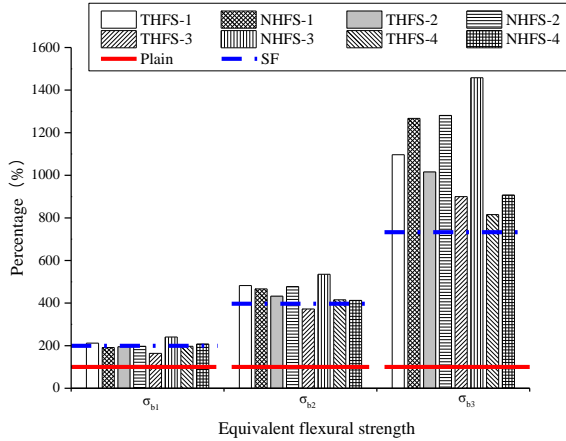


Fig. 10 Comparison of equivalent flexural strength of Plain, SF, THFS and NHFS groups

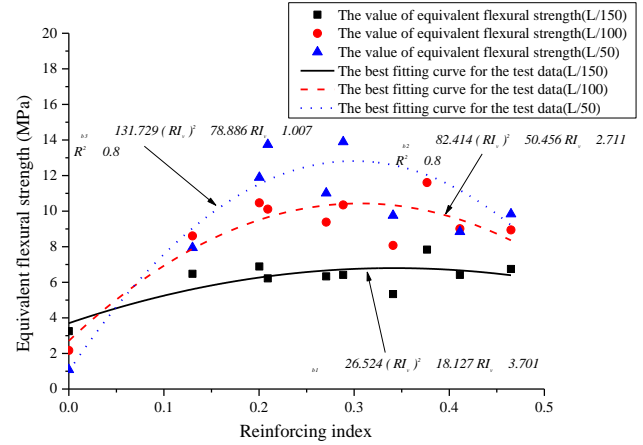


Fig. 11 Relationship between reinforcing index and equivalent flexural strength

hybrid fiber start a synergy effect after the matrix cracking. The NHFS-3 has the best energy absorption capacity among all groups.

The equivalent flexural strength (*EFS*) is residual loading capacity of FRCC for four-point flexural test in JCI-SF4 (1983). The calculation formula of equivalent flexural strength is stated as follows

$$\sigma_b = \frac{T_b L}{\delta_b b h^2} \tag{8}$$

Where, σ_b is the equivalent flexural strength; T_b represent flexural toughness; $L=150$ mm, $\delta_b = L/150, L/100, L/50$ in this study; b and h are the width and height of the specimens, respectively.

The value of *EFS* in specific deflection are shown in Table 6. It may be noted that with increase in specified deflection, the value of *EFS* also increases. The comparison of *EFS* of plain, SF, THFS, NHFS groups are shown in Fig. 10. The toughening of the fiber group increases with increases in deflection. This may be due to that the toughening effect of fiber play more important role in the post-cracking. In comparison to SF group, NHFS-3 group has the highest *EFS* value, the σ_{b1}, σ_{b2} and σ_{b3} of NHFS-3 are increased by 20.9%, 34.9% and 99.0%, respectively. The toughening effect of NHFS-3 is also improved as compared to that of other groups. Compared to the THFS-3 group, the *EFS* value of NHFS-3 increased by 46.8%, 43.7% and 62.1%, respectively. This increases may be due to the resistance against cracking provided by multiscale new hybrid fiber at different scales. However, NHFS-4 group is still not satisfactory, due to the poor dispersion of PVA fiber and excessive CaCO₃ whisker result in heterogeneity and internal defect to matrix.

The relationship between RI_v and *EFS* are presented in Fig. 11. The fitting curves are plotted based on the test data, and regression equations are obtained. The fitting formulas are as follows:

For the fitting curve at $L/150$

$$\sigma_{b1} = -26.524(RI_v)^2 + 18.127RI_v + 3.701 \tag{9}$$

For the fitting curve at $L/100$

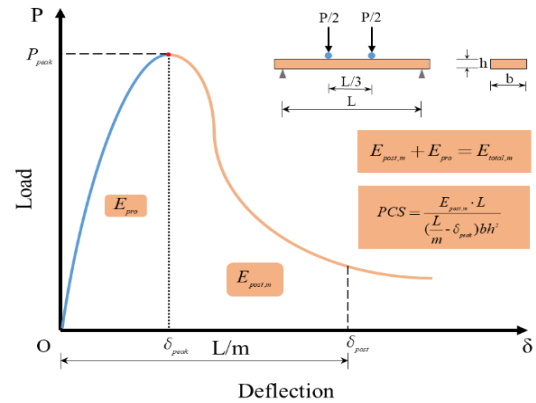


Fig. 12 The technique of PCS

$$\sigma_{b2} = -82.414(RI_v)^2 + 50.456RI_v + 2.711 \tag{10}$$

For the fitting curve at $L/50$:

$$\sigma_{b3} = -131.729(RI_v)^2 + 78.886RI_v + 1.007 \tag{11}$$

3.4.3 Evaluation of flexural toughness based on post-crack strength (PCS)

A large number of researches concentrate on the flexural toughness test methods of ASTM C1018 and JCI-SF4 standard. However, these two standardized test methods exist imperfection up to some extent (Banthia and Trottier 1995). The values of toughness can't be determined accurately, since the method to determine the occurrence of first crack has occasionality in ASTM C1018 and it is difficult to make a field performance of FRCC. The the technique of JCI-SF4 always be criticized for that the span/150 deflection is too far to be affected by the instability in the initial portion. Meanwhile, flexural toughness factors directly depend upon the geometrical variables associated with the specimen and the loading arrangement. In this work, a new method is used to evaluate the flexural toughness and energy absorption capacity which was proposed by Banthia (Soleimani and Banthia 2005, Banthia and Trottier 1995). The schematic diagram of PCS technique is shown in Fig. 12. The Eq. (12) for PCS as

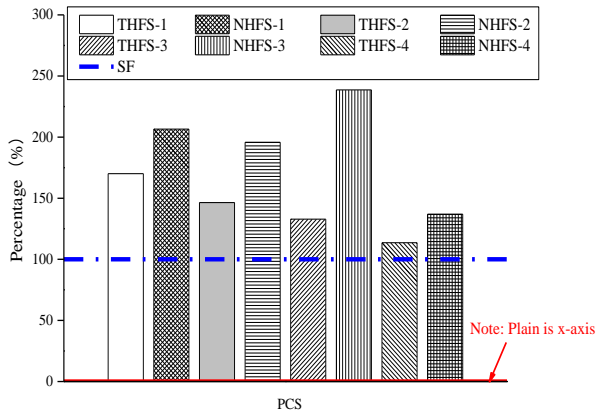


Fig. 13 Comparison of PCS of plain, SF, THFS and NHFS groups

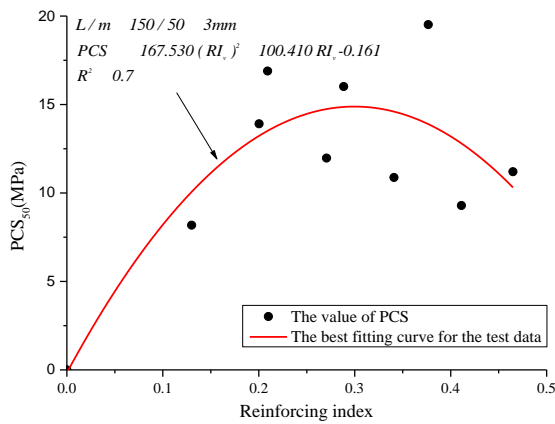


Fig. 14 Relationship between reinforcing index and PCS

the index of evaluation is given as follows

$$PCS = \frac{E_{post,m} \cdot L}{\left(\frac{L}{m} - \delta_{peak}\right)bh^2} \quad (12)$$

Where $E_{post,m}$ is equal to the total energy ($E_{total,m}$) minus the pre-peak energy (E_{pre}); L is span of specimens; δ_{peak} is the value of deflection which is corresponding to ultimate load; The value of m in Eq. (12) is chosen depending on the application according to (Banthia and Trottier 1995). In this paper, the L/m equal to 3 when m is taken as 50. It can be seen from Figs. 5 and 12 that $L/m=3$ can maximum evaluate the PCS values of all curves; Where b and h are the width and height of the specimens, respectively.

The comparison of plain, SF, THFS, NHFS groups are shown in Fig. 13. The PCS value of plain group is on x-axis (zero), because of brittle failure of plain group, there is no post-crack strength. The value of PCS of THFS-1, THFS-2, THFS-3, THFS-4, NHFS-1, NHFS-2, NHFS-3 and NHFS-4 are improved by 70.0%, 46.4%, 32.9%, 13.6%, 106.5%, 95.8%, 138.6% and 36.9%, respectively, as compared to that of SF group. The NHFS have higher PCS value than that of THFS. The PCS value of NHFS-1, NHFS-2, NHFS-3 and NHFS-4 groups are improved by 21.4%, 33.8%, 79.5% and 20.6%, respectively, as compared to that of THFS-1, THFS-2, THFS-3 and THFS-4, respectively.

Among of the NHFS, NHFS-3 group has the best PCS. The 1.25% steel fiber, 0.55% PVA fiber and 2% $CaCO_3$ whisker are the best combination of NHFS-3 group which make a positive hybrid effect and can restrict crack at different scales up to some extent.

As shown in Fig. 14, the type of fitting curve is similar to previous fitting curve (Fig. 9 and Fig. 11), and it certify the evaluation consistency of PCS technique to contrast with ASTM C1018 and JCI-SF4. The correlation coefficient is equal to 0.7 which lower than others, but here in particular NHFS-3 still possess the best flexural toughness. The fitting formulas is as follows

$$PCS = -167.530 (RI_v)^2 + 100.410 RI_v - 0.161 \quad (13)$$

3.5 Micro-morphological characteristics

After the flexural test, the micro-morphological characteristics of NHFS group is observed by scanning electron microscopy. There exists different micro-morphological characteristics under different magnifications as shown in Fig. 15. From Fig. 15(a)-(b) the well-dispersed steel fiber, PVA fiber and $CaCO_3$ whisker can be seen in the matrix and has strong bond capacity among them. Hence, this behavior can help to resist the cracking. Fig. 15(c)-(d) shows that the PVA fiber was pulled out of the matrix and leave a hole with slip trace. Since, PVA fiber is the hydrophilic material which concludes that the process of polyvinyl alcohol fiber was pulled out which take great deal of energy thereby improving flexural toughness. By magnifying sample to 2500 times and 4000 times as shown in Fig. 15(e)-(f), the micro-morphological characteristics of $CaCO_3$ whisker can be noticed. The whisker stride over the crack and play a good bridging effect in Fig. 15(e)-(f). It shows the effect of crack arresting at micro-scale level. The slip trace of whisker in Fig. 15(f) further proved the function in restricting the cracking propagation at microscopic area. By summarizing the photos of micro-morphological in Fig. 15, it can be concluded that steel fiber, polyvinyl alcohol fiber and $CaCO_3$ whisker can make an effectively collaboration with each other and produce good toughening and reinforcing actions at different scales in NHFS group

4. Discussion

The new hybrid fiber system (NHFS) which the addition of $CaCO_3$ whisker to steel-PVA hybrid fiber reinforced cementitious composites can improve the flexural performance as compared to that of traditional hybrid fiber system (THFS). The NHFS-1, NHFS-2 and NHFS-3 has more extended softening branch and deflection capacity after peak load than that of THFS-1, THFS-2 and THFS-3, respectively. However, NHFS-4 which have 3.0% volume fraction of $CaCO_3$ whisker is not good as compared to that of NHFS-1, NHFS-2 and NHFS-3. This demonstrates that excess $CaCO_3$ whisker would reduce flexural performance. The reinforcement effect of hybrid fiber groups was present not only improve deflection at first crack point but also at peak load point as compared with plain and SF groups. This

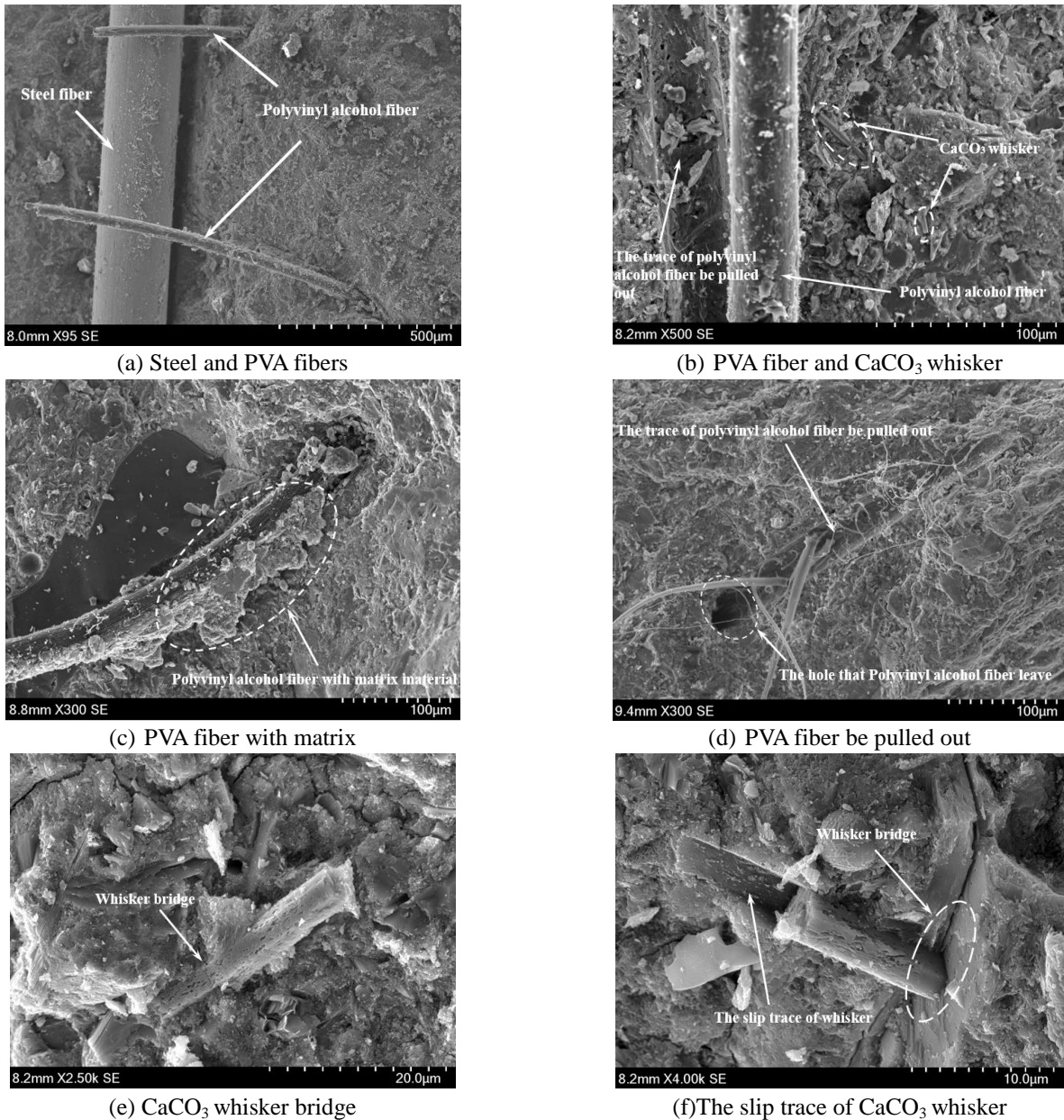


Fig. 15 The Micro-morphological characteristics of NHFS group

shows that hybrid fiber has a multiscale crack arresting effect. Meanwhile, NHFS show a better flexural strength than THFS. Because of the addition of CaCO₃ whisker in THFS make a positive hybrid effect to fill matrix and limit the generation, development and propagation of cracks at different scales. And the trend of fitting curve about reinforcing index (RI_v) and relative increase ratio of first crack strength or ultimate strength indicate that moderate fiber content or aspect ratio value can improve strength, but excessive content result in decreased strength.

By using ASTM C1018 standard, JCI-SF4 standard and post-crack strength (PCS) techniques the empirical relationship between RI_v and evaluation parameters of flexural toughness are discussed. The best fitting curve of RI and toughness index (TI) analyzed in the experiment results shows that with increase in the RI_v , the TI value is also increase first and then decrease in the groups with

CaCO₃ whisker having higher TI than others, except NHFS-4. This means that NHFS have better energy absorption capacity in post-crack stage with optimum dosage of CaCO₃ whiskers. Similarly, with the increase in RI_v , the equivalent flexural strength and PCS also exhibit the similar tendency, and NHFS-3 have overall best performance. The regression equations and quantitative correlation coefficients reflect the relationship between reinforcing index and evaluation parameters of flexural toughness. The fitting results in this study indicate that the mathematical formula of RI_v can give expression to the toughening effect of the hybrid system and have a good applicability.

The observation of micro-morphology verify the NHFS could play a role in toughening and reinforcing effect to cement matrix at different scales. The optimum CaCO₃ whisker content into traditional hybrid fiber cementitious composites can remarkable improve the flexural properties

of slabs. The NHFS-3 (1.25% steel fiber+0.55% PVA fiber +2% CaCO₃ whisker) is the best group and make an optimum positive hybrid effect. The steel fiber, PVA fiber and CaCO₃ whisker are multiscale fiber and play a role in restricting cracking process at different scales to achieve reinforcing and toughening. The steel and PVA fibers arresting cracks from meso-level to macro-level (Zhang and Cao 2017). The CaCO₃ whisker fill the pores and improve the compactness of matrix, and can control the propagation of micro-cracks by whisker bridging, crack deflection, whisker pulled out. The new hybrid fiber reinforced cementitious composites further improved the flexural strength, flexural toughness and crack resistance capacity ultimately enhance the durability of structures. Based on the above result, the NHFS can improve the flexural performance of slab. Thus, favoring the utility of NHFS with optimum content for the structural applications.

5. Conclusions

In this study, the flexural properties of slab with new hybrid fiber system (NHFS) are investigated for slab application. The flexural strength, toughness index(*TI*), equivalent flexural strength (*EFS*) and post-crack strength (*PCS*) are studied in detail. Following conclusions are made:

- According to the flexural parameter of ASTM C1018, in comparison to plain and steel fiber groups, the *TI* values of NHFS groups improved by 427% - 697% and 33% - 101%, respectively.
- Based on JCI-SF4, compared to plain and steel fiber group, the value of *EFS* of NHFS groups are increased by 807% -1358% and 24% - 99%, respectively, at *L/50* deflection.
- In comparison to steel fiber group, there is an increase of 37% - 139% in *PCS* of NHFS groups.
- The relationship between reinforcing index (*RI_v*) and flexural parameters shows that, as the value of *RI_v* increases different flexural parameters increases; but then decreases indicating existence of optimal values of *RI_v* corresponding to the best flexural parameters. The optimum *RI_v* values calculated using fitting equations, can be used to guide the mix design of steel-PVA fibers-CaCO₃ whisker composites to achieve the best flexural properties of slabs.
- The micro-morphological characteristics of NHFS indicate that CaCO₃ whisker play an improvement role in toughening and reinforcing effect at different level with steel-PVA fibers in cementitious composites.

Hence, the enhanced flexural properties of slab with new hybrid fiber reinforced cementitious composites are favoring its utility for structural application. The new hybrid fiber system can be helpful in improving the performance of bridge decks, connecting slabs of bridge, repair of structural components and protective outer walls.

Acknowledgments

The authors would like to acknowledge the support of

this work by the Natural Science Foundation of China under Grant NO.51678111 and NO.51478082. The authors are also thankful to China Scholarship Council (CSC) for providing financial support for PhD studies of Engr. Mehran Khan at Dalian University of Technology, Dalian, China.

Reference

- Abadel, A.A. (2015), "Mechanical properties of hybrid fibre-reinforced concrete-analytical modelling and experimental behavior", *Mag. Concrete Res.*, **68**(16), 823-843.
- Ahmed, S.F.U., Maalej, M. and Paramasivam, P. (2007), "Flexural responses of hybrid steel-polyethylene fiber reinforced cement composites containing high volume fly ash", *Constr. Build. Mater.*, **21**(5), 1088-1097.
- Alberti, M.G., Enfedaque, A. and Gálvez, J.C. (2016), "Fracture mechanics of polyolefin fibre reinforced concrete: study of the influence of the concrete properties, casting procedures, the fibre length and specimen size", *Eng. Fract. Mech.*, **154**, 225-244.
- Almusallam, T., Ibrahim, S.M., Al-Salloum, Y., Abadel, A. and Abbas, H. (2016), "Analytical and experimental investigations on the fracture behavior of hybrid fiber reinforced concrete", *Cement Concrete Compos.*, **74**, 201-217.
- Arslan, M.E. (2016), "Effects of basalt and glass chopped fibers addition on fracture energy and mechanical properties of ordinary concrete: cmod measurement", *Constr. Build. Mater.*, **114**, 383-391.
- ASTM C 1018 (1997), Standard Test Method for Flexural Toughness and First Crack Strength of Fiber Reinforced Concrete (using Beam with Third-point Loading), American Society for Testing and Materials, West Conshohocken, PA.
- ASTM C1609/1609M (2012), Standard Test Method for Flexural Performance of Fiber-reinforced Concrete (using Beam with Third-point Loading), American Society for Testing and Materials, West Conshohocken, PA.
- Atahan, H.N., Tuncel, E.Y. and Pekmezci, B.Y. (2013), "Behavior of pva fiber-reinforced cementitious composites under static and impact flexural effects", *J. Mater. Civil Eng.*, **25**(10), 1438-1445.
- Banthia, N. and Trottier, J.F. (1995), "Test methods for flexural toughness characterization of fiber reinforced concrete: some concerns and a proposition", *ACI Mater. J.*, **92**(1), 48-57.
- Cao, M. and Li, L. (2018), "New models for predicting workability and toughness of hybrid fiber reinforced cement-based composites", *Constr. Build. Mater.*, **176**, 618-628.
- Cao, M., Li, L., Li, Z. and Si, W. (2017), "Influence of CaCO₃ whisker on flexural behavior of steel-polyvinyl alcohol hybrid fiber reinforced cement-based composite slabs", *Acta Materialia Sinica*, **11**(34), 2614-2623.
- Cao, M., Zhang, C. and Lv, H. (2014b), "Mechanical response and shrinkage performance of cementitious composites with a new fiber hybridization", *Constr. Build. Mater.*, **57**(5), 45-52.
- Cao, M., Zhang, C. and Wei, J. (2013), "Microscopic reinforcement for cement based composite materials", *Constr. Build. Mater.*, **40**(3), 14-25.
- Cao, M., Zhang, C., Li, Y. and Wei, J. (2015), "Using calcium carbonate whisker in hybrid fiber-reinforced cementitious composites", *J. Mater. Civil Eng.*, **27**(4), 04014139.
- Cao, M., Zhang, C., Lv, H. and Xu, L. (2014a), "Characterization of mechanical behavior and mechanism of calcium carbonate whisker-reinforced cement mortar", *Constr. Build. Mater.*, **66**(1), 89-97.
- Cao, P., Feng, D., Zhou, C. and Zuo, W. (2014), "Study on fracture behavior of polypropylene fiber reinforced concrete with

- bending beam test and digital speckle method”, *Comput. Concrete*, **14**(5), 527-546.
- CECS38 (2004), Technical Specification for Fiber Reinforced Concrete Structures, China Association for engineering construction standardization, China Architecture & Building Press, Beijing, China.
- Demir, A. (2015), “Prediction of hybrid fibre-added concrete strength using artificial neural networks”, *Comput. Concrete*, **15**(4), 503-514.
- JCI-SF4 (1983), JCI Standards for Test Methods of Fiber Reinforced Concrete, Methods of Tests for Flexural Strength and Flexural Toughness of Fiber Reinforced Concrete, Japan Concrete Institute.
- Kazemi, M.T., Golsorkhtabar, H., Beygi, M.H.A. and Gholamitabar, M. (2017), “Fracture properties of steel fiber reinforced high strength concrete using work of fracture and size effect methods”, *Constr. Build. Mater.*, **142**, 482-489.
- Khan, M. and Ali, M. (2016), “Use of glass and nylon fibers in concrete for controlling early age micro cracking in bridge decks”, *Constr. Build. Mater.*, **125**, 800-808.
- Kim, J.S., Lee, H.J. and Choi, Y. (2013), “Mechanical properties of natural fiber-reinforced normal strength and high-fluidity concretes”, *Comput. Concrete*, **11**(6), 531-539.
- Lawler, J.S., Zampini, D. and Shah, S.P. (2016), “Microfiber and macrofiber hybrid fiber-reinforced concrete”, *J. Mater. Civil Eng.*, **17**(5), 595-604.
- Li, V. (2007), “Progress and application of engineered cementitious composites”, *J. Chin. Ceramic Soc.*, **35**(4), 531-536.
- Najigivi, A., Nazerigivi, A. and Nejati, H.R. (2017), “Contribution of steel fiber as reinforcement to the properties of cement-based concrete: a review”, *Comput. Concrete*, **20**(2), 155-164.
- Pereira, E.B., Fischer, G. and Barros, J. (2012), “Effect of hybrid fiber reinforcement on the cracking process in fiber reinforced cementitious composites”, *Cement Concrete Compos.*, **34**(10), 1114-1123.
- Pichler, C., Lackner, R. and Mang, H.A. (2008), “Multiscale model for creep of shotcrete - from logarithmic-type viscous behavior of csh at the. mu.m-scale to macroscopic tunnel analysis”, *J. Adv. Concrete Technol.*, **6**(1), 91-110.
- Qian, C. and Stroeven, P. (2000), “Fracture properties of concrete reinforced with steel- polypropylene hybrid fibres”, *Cement Concrete Compos.*, **22**(5), 343-351.
- Said, S.H. and Razak, H.A. (2015b), “The effect of synthetic polyethylene fiber on the strain hardening behavior of engineered cementitious composite (ecc)”, *Mater. Des.*, **86**, 447-457.
- Said, S.H., Razak, H.A. and Othman, I. (2015a), “Flexural behavior of engineered cementitious composite (ECC) slabs with polyvinyl alcohol fibers”, *Constr. Build. Mater.*, **75**, 176-188.
- Soleimani, S.M. and Banthia, N. (2005), “Flexural response of hybrid fiber-reinforced cementitious composites”, *ACI Mater. J.*, **102**(6), 382-389.
- Sun, W., Chen, H., Luo, X. and Qian, H. (2001), “The effect of hybrid fibers and expansive agent on the shrinkage and permeability of high-performance concrete”, *Cement Concrete Res.*, **31**(4), 595-601.
- Tuan, B.L.A., Tesfamariam, M.G., Hwang, C.L., Chen, C.T., Chen, Y.Y. and Lin, K.L. (2014), “Effect of fiber type and content on properties of high-strength fiber reinforced self-consolidating concrete”, *Comput. Concrete*, **14**(3), 299-313.
- Yun, H.D., Fukuyama, H., Jeon, E., Yang, I.S., Choi, C.S. and Kim, S.W. (2007), “Mechanical properties of high-performance hybrid-fiber-reinforced cementitious composites (HPHFRCCs)”, *Mag. Concrete Res.*, **59**(4), 257-271.
- Zhang, C. and Cao, M. (2014), “Fiber synergy in multi-scale fiber-reinforced cementitious composites”, *J. Reinf. Plast. Compos.*, **33**(9), 862-874.
- Zhang, J., Wang, Q. and Wang, Z. (2017), “Properties of polyvinyl alcohol-steel hybrid fiber reinforced composite with high-strength cement matrix”, *J. Mater. Civil Eng.*, **29**(7), 04017026.

CC